Archival Report

Episodic Memory–Related Imaging Features as Valuable Biomarkers for the Diagnosis of Alzheimer's Disease: A Multicenter Study Based on Machine Learning

Yachen Shi, Zan Wang, Pindong Chen, Piaoyue Cheng, Kun Zhao, Hongxing Zhang, Hao Shu, Lihua Gu, Lijuan Gao, Qing Wang, Haisan Zhang, Chunming Xie, Yong Liu, and Zhijun Zhang, for the Alzheimer's Disease Neuroimaging Initiative

ABSTRACT

BACKGROUND: Individualized and reliable biomarkers are crucial for diagnosing Alzheimer's disease (AD). However, lack of accessibility and neurobiological correlation are the main obstacles to their clinical application. Machine learning algorithms can effectively identify personalized biomarkers based on the prominent symptoms of AD.

METHODS: Episodic memory–related magnetic resonance imaging (MRI) features of 143 patients with amnesic mild cognitive impairment (MCI) were identified using a multivariate relevance vector regression algorithm. The support vector machine classification model was constructed using these MRI features and verified in 2 independent datasets ($N = 994$). The neurobiological basis was also investigated based on cognitive assessments, neuropathologic biomarkers of cerebrospinal fluid, and positron emission tomography images of amyloid-β plaques.

RESULTS: The combination of gray matter volume and amplitude of low-frequency fluctuation MRI features accurately predicted episodic memory impairment in individual patients with amnesic MCI ($r = .638$) when measured using an episodic memory assessment panel. The MRI features that contributed to episodic memory prediction were primarily distributed across the default mode network and limbic network. The classification model based on these features distinguished patients with AD from normal control subjects with more than 86% accuracy. Furthermore, most identified episodic memory–related regions showed significantly different amyloid-β positron emission tomography measurements among the AD, MCI, and normal control groups. Moreover, the classification outputs significantly correlated with cognitive assessment scores and cerebrospinal fluid pathological biomarkers' levels in the MCI and AD groups.

CONCLUSIONS: Neuroimaging features can reflect individual episodic memory function and serve as potential diagnostic biomarkers of AD.

Alzheimer's disease (AD) is a neurodegenerative disease characterized by the accumulation of amyloid-β (Aβ) plaques and neurofibrillary tangles in the brain (1). Individuals with mild cognitive impairment (MCI), especially amnesic MCI (aMCI), are at higher risk of progressing to AD (2). The A/T/N (β amyloid/pathological tau/neurodegeneration) research framework includes cerebrospinal fluid (CSF) and molecular positron emission tomography (PET) imaging biomarkers (3), emphasizing the importance of reliable biomarkers for diagnosing AD. However, the high invasiveness and costs of these approaches limit their widespread use and potential in screening patients for AD. Therefore, it is crucial to identify novel, accessible, and individualized diagnostic biomarkers for AD.

Episodic memory refers to the ability to record, retain, and recognize spatiotemporal information based on personal experiences and is characteristically impaired during AD (4,5).

Magnetic resonance imaging (MRI) is a noninvasive means for detecting changes in brain function (6,7). In a previous study, we found that the functional connectivity (FC) of the hippocampal subregion with the prefrontal, temporal, and parietal lobes was significantly decreased in patients with aMCI, indicating that episodic memory deficit may be directly associated with impaired hippocampal function (8). Furthermore, several meta-analyses have reported a significant association of the medial temporal lobe, including hippocampal and parahippocampal gyri and the entorhinal cortex, with episodic memory recording and retrieval (9,10). In addition, the prefrontal cortex, parietal cortex, and occipital cortex are activated during encoding and recalling and interact with the medial temporal lobe to establish the core network of episodic memory processing (10,11). However, studies on the association between episodic memory and neuroimaging biomarkers

have been largely based on the group-level rather than individual statistics, which has limited utility in clinical practice.

Multivariate machine learning regression algorithms have successfully decoded continuous clinical assessments from neuroimaging scans at the single-subject level. Neuroimaging studies use multiple algorithms, including linear support vector regression (12), ridge regression (13), and relevance vector regression (RVR) (14,15), which show similar predictive performance. RVR has the following advantages over other equivalent algorithms: 1) selection of fewer relevance vectors, which reduces model complexity and computational cost and increases predictive efficacy, and 2) absence of within-algorithm parameters that obviate additional computation for parameter optimization (16–18). Furthermore, the support vector machine (SVM) can recognize subtle patterns from complex datasets and is the most widely used supervised learning method for building classification models (19).

To date, multiple machine learning models have been built based on the MRI data in public AD-related datasets in hundreds of published studies, in which the use of deep learning or modified machine learning algorithms helped obtain better classification or prediction performance (20–22). However, fewer studies have constructed and validated such models using several independent, multicenter datasets (23–40). The primary challenge in the clinical use of machine learning models is the poor generalizability and repeatability among different cohorts. Therefore, independent, multicenter dataset cross-validation is essential for translation medicine.

In this study, we identified episodic memory–related neuroimaging biomarkers using the RVR method and investigated the clinical value of these biomarkers (Figure 1). Briefly, the episodic memory impairment that was measured by an episodic memory assessment panel in individual patients with aMCI were quantified using MRI data, and episodic memory–related features with accurate predictions were selected for building the SVM model for classifying patients with aMCI from normal control (NC) subjects. The classification model was validated on patients with MCI/AD and NC subjects in two independent, multicenter datasets, and the specificity was determined by testing on patients with major depressive disorder and NC subjects. Furthermore, cognitive assessments, CSF Aβ42 and total tau levels, and Aβ PET measurements were also analyzed to determine a possible neurological basis of the episodic memory–related features and classification outputs.

METHODS AND MATERIALS

Participants

Discovery Dataset for Building Models: ZhongDa Hospital Dataset. A total of 143 patients with aMCI and 178
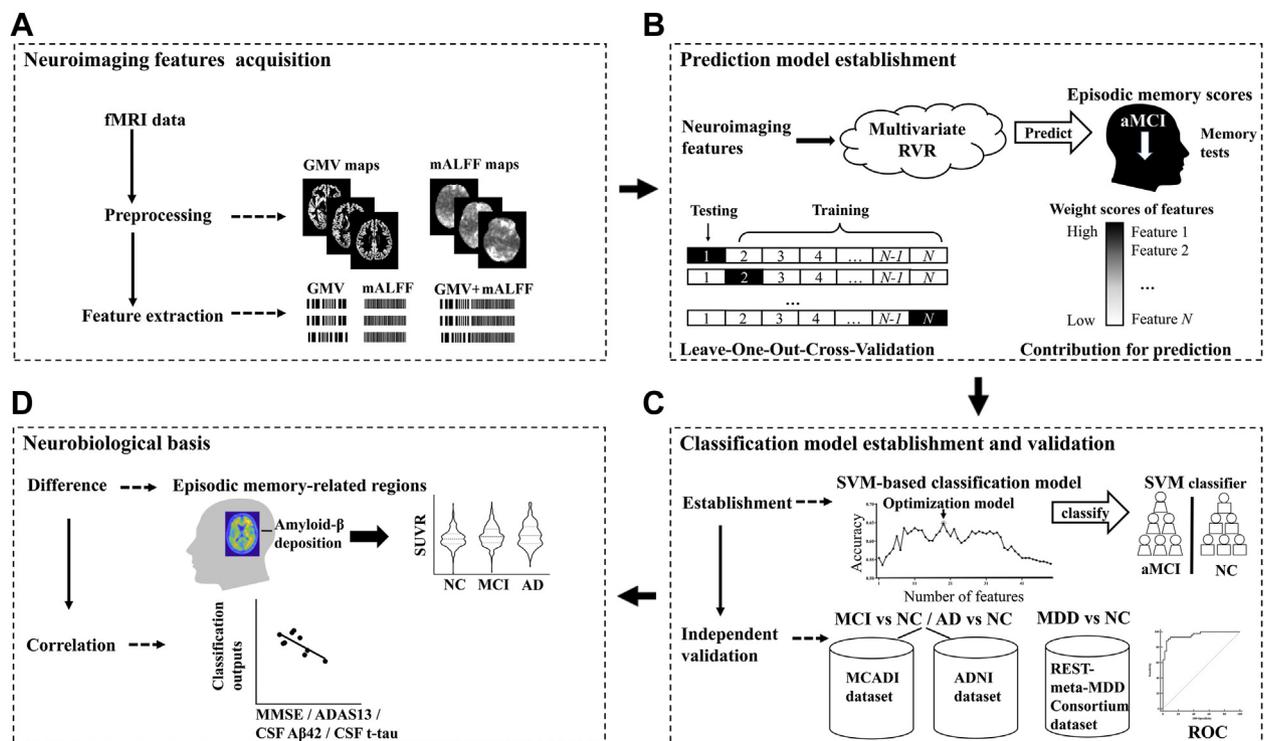

Figure 1. Schematic of the data analysis pipeline. **(A)** Imaging data preprocessing and feature extraction with each brain region based on the Brainnetome atlas. **(B)** Overview of the relevance vector regression (RVR) prediction framework in patients with amnesic mild cognitive impairment (aMCI). **(C)** Establishment and validation of episodic memory–related support vector machine (SVM) classification model. **(D)** Exploration of the neurobiological basis. Aβ, amyloid-β; AD, Alzheimer's disease; ADAS13, Alzheimer's Disease Assessment Scale 13-item Cognitive Subscale; ADNI, Alzheimer's Disease Neuroimaging Initiative; CSF, cerebrospinal fluid; fMRI, functional magnetic resonance imaging; GMV, gray matter volume; mALFF, mean amplitude of low-frequency fluctuation; MCADI, Multi-Center Alzheimer Disease Imaging; MDD, major depressive disorder; MMSE, Mini-Mental State Examination; NC, normal control; ROC, receiver operating characteristic; SUVR, standardized update value ratio; t-tau, total tau.

Episodic Memory–Related Imaging Features of AD

NC subjects were recruited from the Affiliated ZhongDa Hospital of Southeast University following approval of the ethics committee. All participants or their legal guardians provided signed consent forms before the start of the study. Global cognition was assessed using the Mini-Mental State Examination (MMSE) (41), and episodic memory function was assessed using the Auditory Verbal Learning Test 20-minute Delayed Recall (42), Logical Memory Test 20-minute Delayed Recall (43), and Rey-Osterrieth Complex Figure Test 20-minute Delayed Recall (44). Detailed information is summarized in Table 1 and the Supplement. All participants also underwent multimodal MRI, and the acquisition protocol is outlined in Table S1.

As described previously (45,46), the raw scores of each test were initially transformed to z scores using the corresponding mean and standard deviation, and the individual episodic memory scores were calculated using the z-transformed average of the relevant cognitive tests. Additional details are provided in the Supplement.

Validation Dataset for Testing Models: Multi-Center Alzheimer Disease Imaging Consortium Dataset. The Multi-Center Alzheimer Disease Imaging (MCADI) dataset included 687 participants (252 AD, 220 MCI, and 215 NC) from 6 datasets (Table 1 and Supplement) (47). MRI for these participants was acquired from 6 different scanners (Supplement and Table S1).

Validation Dataset for Testing Models: Alzheimer's Disease Neuroimaging Initiative Dataset. The Alzheimer's Disease Neuroimaging Initiative (ADNI) dataset (www.loni.ucla.edu/ADNI) comprised 1077 participants (291 AD, 452 MCI, and 334 NC) with Aβ PET images, part of which had been

used in our previous study (48). The structural MRI and resting-state functional MRI data, MMSE and Alzheimer's Disease Assessment Scale 13-item Cognitive Subscale evaluations, and CSF Aβ42 and total tau measurements were available for 307 of these participants (53 AD, 149 MCI, and 105 NC). Clinical details are provided in Table 1 and Table S2. The imaging acquisition protocol is outlined in Table S1.

Validation Dataset for Testing Models: REST-meta-MDD Consortium Dataset. This dataset was obtained from 25 research groups across 17 Chinese hospitals, and the largest dataset with 248 patients with major depressive disorder and 251 NC subjects was used in the present study (49). The patient details are summarized in Table 1 and the Supplement, and imaging acquisition parameters are presented in Table S1.

PET Imaging in the ADNI Dataset

The PET methodology has been previously described (50). Standardized update value ratios (SUVRs) were calculated with a standardized cortical anatomical automatic labeling volume-of-interest template placed on spatially normalized image volumes using a whole-cerebellum reference region. SUVRs of all brain regions were subsequently obtained based on the Brainnetome Atlas (Table S3) (51).

Image Acquisition and Preprocessing

Data acquisition and preprocessing for each dataset have been described in detail in our previous studies (48,52) and the Supplement. The average modulate gray matter volume (GMV) values of 210 cortical and 36 subcortical subregions (Table S3), as described in the Brainnetome Atlas (51), were

Table 1. Demographic and Neuropsychological Data of Subjects

Dataset	Group	n	Age, Years	Sex, M/F	Global Assessments[a]	AVLT-20-min-DR z Scores	ROCFT-20-min-DR z Scores	LMT-20-min-DR z Scores	Episodic Memory z Scores
ZhongDa Hospital Dataset	NC	178	66.51 ± 7.31	84/94	28.33 ± 1.36	0.76 ± 0.62	0.43 ± 0.80	0.44 ± 0.89	0.54 ± 0.52
	aMCI	143	66.78 ± 7.53	66/77	27.04 ± 1.79	−0.94 ± 0.40	−0.53 ± 0.96	−0.55 ± 0.85	−0.67 ± 0.59
MCADI Consortium Dataset	NC	215	66.67 ± 6.57	84/131	28.44 ± 1.73	–	–	–	–
	MCI	220	68.35 ± 9.21	101/119	24.94 ± 3.48	–	–	–	–
	AD	252	68.58 ± 8.29	105/147	16.61 ± 6.17	–	–	–	–
ADNI Dataset (PET Analysis)	NC	334	73.78 ± 6.01	167/167	29.10 ± 1.21	–	–	–	–
	MCI	452	73.48 ± 6.63	272/180	27.83 ± 2.00	–	–	–	–
	AD	291	74.69 ± 7.26	173/118	21.49 ± 4.37	–	–	–	–
ADNI Dataset (MRI Analysis)	NC	105	72.69 ± 5.61	43/62	28.96 ± 1.14	–	–	–	–
	MCI	149	73.25 ± 6.60	85/64	27.11 ± 2.39	–	–	–	–
	AD	53	73.89 ± 6.85	27/26	21.89 ± 2.80	–	–	–	–
REST-meta-MDD Consortium Dataset	NC	251	39.64 ± 15.87	87/164	–	–	–	–	–
	MDD	248	38.85 ± 13.38	85/163	21.35 ± 4.98	–	–	–	–

Data are presented as mean ± SD or n.

AD, Alzheimer's disease; ADNI, Alzheimer's Disease Neuroimaging Initiative; aMCI, amnesic mild cognitive impairment; AVLT-20-min-DR, Auditory Verbal Learning Test 20-minute Delayed Recall; F, female; LMT-20-min-DR, Logical Memory Test 20-minute Delayed Recall; M, male; MCADI, Multi-Center Alzheimer Disease Imaging; MCI, mild cognitive impairment; MDD, major depressive disorder; MRI, magnetic resonance imaging; NC, normal control; PET, positron emission tomography; ROCFT-20-min-DR, Rey-Osterrieth Complex Figure Test 20-minute Delayed Recall.

[a]Mini-Mental State Examination scale was used for assessing patients with aMCI or MCI and patients with AD, and 17-Item Hamilton Rating Scale for Depression was used for assessing patients with MDD.

extracted for each subject. Besides, the average amplitude of low frequency fluctuation (ALFF), across the 0.01–0.08 frequency band, was computed within each voxel, and the ALFF of each voxel was divided by the global mean ALFF (mALFF) value for each subject, providing mALFF spatial maps (53). Subsequently, for each subject, mALFF values of the above-mentioned 246 brain regions (Table S3) in the Brainnetome Atlas (51) were also extracted. As a result, the GMV and mALFF values were used as feature vectors to perform subsequent analyses.

Multivariate RVR Analysis in Patients With aMCI in the Discovery Dataset

The association between episodic memory scores and GMV and mALFF values was analyzed using multivariate RVR (16) with a linear kernel as implemented in PRoNTo (http://www.mlnl.cs.ucl.ac.uk/pronto/) running under MATLAB (The MathWorks, Inc., Natick, MA) (Supplement). Leave-one-out cross-validation was performed to estimate the generalizability of the model (14,17). The Pearson correlation coefficient (r) and mean absolute error (MAE) between actual and predicted episodic memory scores were used to assess the prediction performance (14,54), and the significance was determined using a permutation test whereby the input-target data were randomly reassigned and the RVR was repeated 1000 times. Subsequently, the distribution of correlation coefficients and MAE values was obtained, and the p value was calculated by dividing the number of times the permuted value was greater (or less) than or equal to the true value by 1000. Furthermore, the absolute value of the weight of each feature was used to quantify its predictive contribution (14,55), and a feature was selected if that value was in the top 10%. This threshold can eliminate noise components to some extent, thus enabling better visualization of the most predictive features. The use of different types of features together in the model may improve prediction performance; therefore, composite MRI features were also analyzed by combining the GMV and mALFF features that were in the top 10% absolute weight scores of the respective RVR model.

SVM Classification

The LIBSVM toolbox of MATLAB was used for the SVM-based classification model (56,57). The SVM classifier was built in the discovery dataset and validated using three validation datasets. Leave-one-out cross-validation was used to validate the generalizability of the model (58), and the performance of the latter was assessed in terms of accuracy, sensitivity, specificity, positive predictive value, and negative predictive value. The area under the curve (AUC) of the receiver operating characteristic curve was used to calculate and determine the distinguishing ability of each model. Lastly, the contribution of each feature in the SVM model was calculated based on the respective weights.

The features in the RVR model were used as input features for SVM classification for distinguishing patients with aMCI from NC subjects in the discovery dataset. As some features may not have contributed to the classifier, a selection step feature was introduced. The primary SVM-based model was first constructed using all features and then arranged in descending order of their absolute SVM weight value.

Subsequently, the top N features were selected sequentially to construct a new SVM model for classifying patients with aMCI and NC subjects, and the most accurate SVM model was identified by comparing the accuracies of all SVM models. Lastly, the optimal SVM model was verified in 2 independent datasets.

Statistical Analysis

Statistical analyses were performed using MedCalc Statistical Software version 15.2.2 (MedCalc Software bvba, Ostend, Belgium). Continuous variables were analyzed using the Kruskal-Wallis test based on normal distribution as determined using the Kolmogorov-Smirnov test. Partial correlation analysis was performed to determine the association between the classification outputs and clinical indices by adjusting for age and sex at $p < .05$.

RESULTS

Multivariate RVR Analysis in the Discovery Dataset

The clinical features of the 143 patients with aMCI from the discovery dataset are summarized in Table 1. The application of RVR to the combined GMV and mALFF features allowed individualized prediction of episodic memory scores ($r = .638$, MAE = 0.374, all $p < .001$) (Figure 2A–C), which was more accurate compared with a single metric (GMV: $r = .564$, MAE = 0.402; mALFF: $r = .183$, MAE = 0.504) and the optimal RVR prediction model. Twenty-five GMV features and 25 mALFF features contributed to RVR prediction, mainly localized in the default mode network (DMN), limbic network (LN), and ventral attention network (Figure 2D, E and Table S4).

SVM Analysis

Building and Screening of SVM-Based Models in the Discovery Dataset. To determine whether episodic memory-related features can identify early AD, a primary SVM model was constructed with 50 MRI features derived from the optimal RVR model for classifying the aMCI and NC groups in the discovery dataset (accuracy = 0.517). The model weights of the features are listed in Table S5. The optimal classifier was then identified by sequentially constructing 50 new SVM models as described in Methods and Materials. As shown in Figure S1, the 19th model most accurately distinguished the patients with aMCI from NC subjects (accuracy = 0.651) and was therefore considered to be the optimal classification model. It consisted of 9 GMV features and 10 mALFF features located primarily in the DMN and LN (Figures S2 and S3).

Independent Repeatability Verification in the Validation Datasets. The optimal SVM classification model was validated on the MCI/AD and NC groups in the MCADI dataset (Table 2). It classified the MCI and NC groups with 69.0% accuracy (sensitivity = 83.3%, specificity = 55.0%, AUC = 0.728) (Figure S4A), and AD and NC groups with 86.9% accuracy (sensitivity = 93.0%, specificity = 81.8%, AUC = 0.921) (Figure S4B). In addition, the classification accuracy of the SVM model in the ADNI dataset (Table 2) was 70.5% (sensitivity = 75.2%, specificity = 63.8%, AUC = 0.780) and 87.3% (sensitivity = 91.4%, specificity = 79.3%, AUC = 0.891),
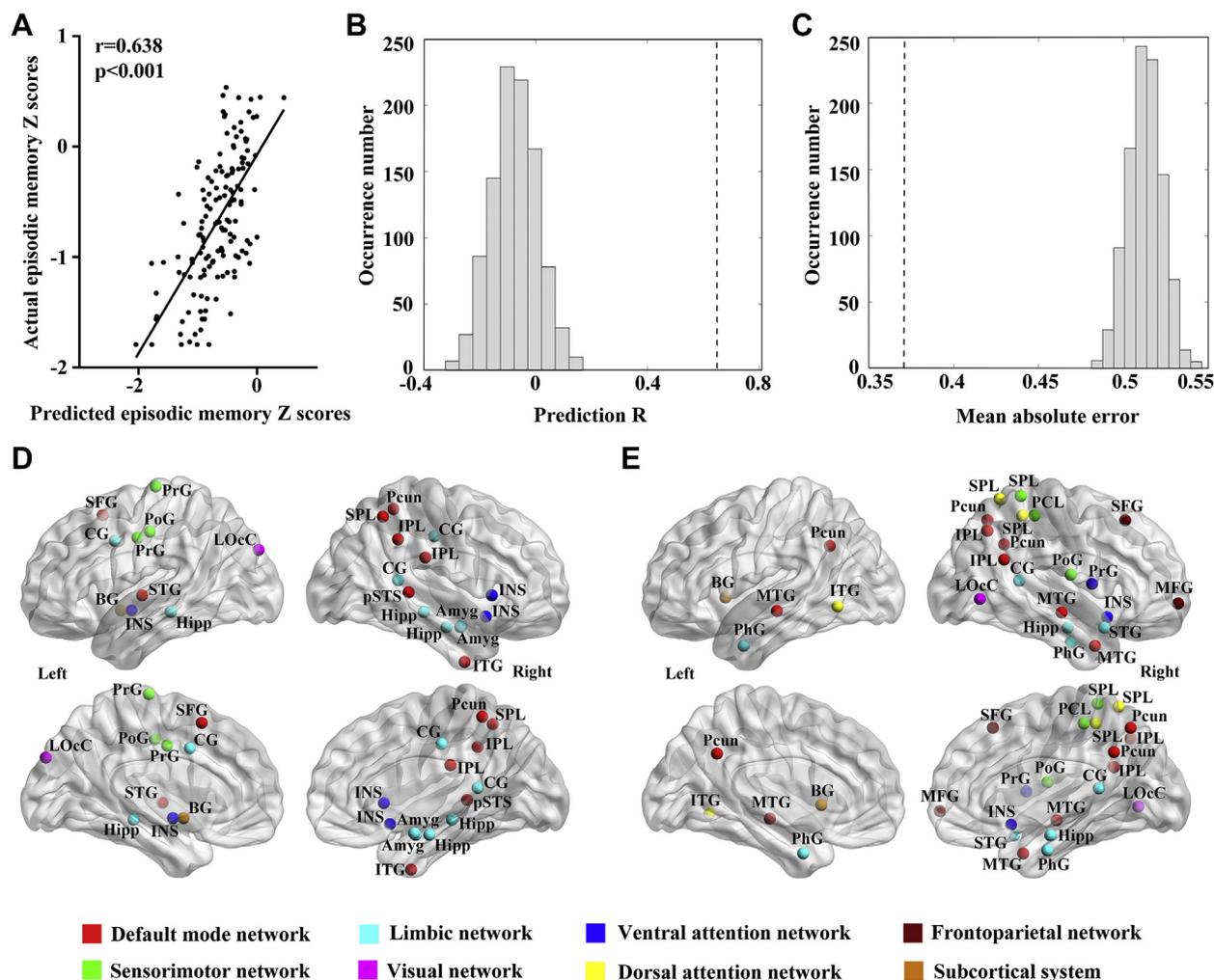
Figure 2. Multivariate relevance vector regression analysis in the discovery dataset. **(A)** Scatterplot showing the predicted episodic memory score for each participant derived from their imaging features compared with their actual episodic memory score. **(B, C)** Distribution of permutation of the prediction *r* and mean absolute error. The values obtained using real scores are indicated by the dashed line. **(D, E)** Visualizations of 25 gray matter volume features and 25 mean amplitude of low-frequency fluctuation features using relevance vector regression analysis for the prediction of episodic memory score. Amyg, amygdala; BG, basal ganglia; CG, cingulate gyrus; Hipp, hippocampus; INS, insular gyrus; IPL, inferior parietal lobule; ITG, inferior temporal gyrus; LOcC, lateral occipital cortex; MFG, middle frontal gyrus; MTG, middle temporal gyrus; PCL, paracentral lobule; Pcun, precuneus; PhG, parahippocampal gyrus; PoG, postcentral gyrus; PrG, precentral gyrus; pSTS, posterior superior temporal sulcus; SFG, superior frontal gyrus; SPL, superior parietal lobule; STG, superior temporal gyrus.

respectively, for classifying patients with MCI and patients with AD from NC subjects (Figure S5).

Specificity Verification in the Validation Dataset. The SVM model was then used on the REST-meta-MDD consortium dataset to differentiate patients with major depressive disorder from NC subjects (Table 2). The classification accuracy was only 51.3% (sensitivity = 47.8%, specificity = 54.8%, AUC = 0.516) (Figure S6).

Exploration of Neuroscientific Interpretability

Neurobiological Basis of Episodic Memory–Related Brain Regions. In the ADNI dataset, among the 47 identified episodic memory–related brain regions (there were 3

overlapping brain regions between the GMV and mALFF features), the SUVRs of 40 regions (approximately 85.1%) were significantly different across the AD, MCI, and NC groups (Table S6). In addition, 15 of the 19 brain regions included in the optimal SVM model also had significantly different SUVRs among 3 groups in the ADNI dataset (Figure S7).

Relationships Between SVM Model Decision Values and Cognitive Ability, Levels of CSF Biomarkers, and Aβ PET SUVRs. The classification outputs and MMSE scores showed significant associations in the MCI and AD groups of the MCADI dataset (Figure 3A, B). Likewise, MMSE and Alzheimer's Disease Assessment Scale 13-item Cognitive Subscale scores showed a significant correlation with the

Table 2. Classification Performance of Proposed 19 Episodic Memory-Related Imaging Features

	ACC	SEN	SPE	PPV	NPV	AUC
MCI vs. NC						
MCADI dataset	0.690	0.833	0.550	0.644	0.771	0.728
ADNI dataset	0.705	0.752	0.638	0.747	0.644	0.780
AD vs. NC						
MCADI dataset	0.869	0.930	0.818	0.813	0.932	0.921
ADNI dataset	0.873	0.914	0.793	0.897	0.824	0.891
MDD vs. NC						
REST-meta-MDD Consortium	0.513	0.478	0.548	0.517	0.509	0.516

ACC, accuracy; AD, Alzheimer's disease; ADNI, Alzheimer's Disease Neuroimaging Initiative; AUC, area under the curve of the receiver operating characteristic; MCADI, Multi-Center Alzheimer Disease Imaging; MCI, mild cognitive impairment; MDD, major depressive disorder; NC, normal control; NPV, negative predictive value; PPV, positive predictive value; SEN, sensitivity; SPE, specificity.

classification outputs in the MCI and AD groups of the ADNI dataset (Figure 3C–F). The classification outputs were significantly correlated with CSF Aβ42 and total tau levels in the MCI group (Figure 3G, H); however, in the AD group the classification outputs were significantly correlated only with CSF Aβ42 levels (Figure 3I, J).

DISCUSSION

In the present study, episodic memory impairment was quantified for individual patients with aMCI using the RVR model, and the distinguishing power, reproducibility, and generalizability of episodic memory–related MRI features were systematically validated in several independent datasets using the SVM method. In addition, the association of these imaging biomarkers with the cognitive and pathological indices of AD was measured to determine their clinical value. We found that the combined use of GMV and mALFF features could predict episodic memory scores of individual patients with aMCI with greater accuracy. Furthermore, an SVM classifier with 19 episodic memory–related MRI features was identified, which
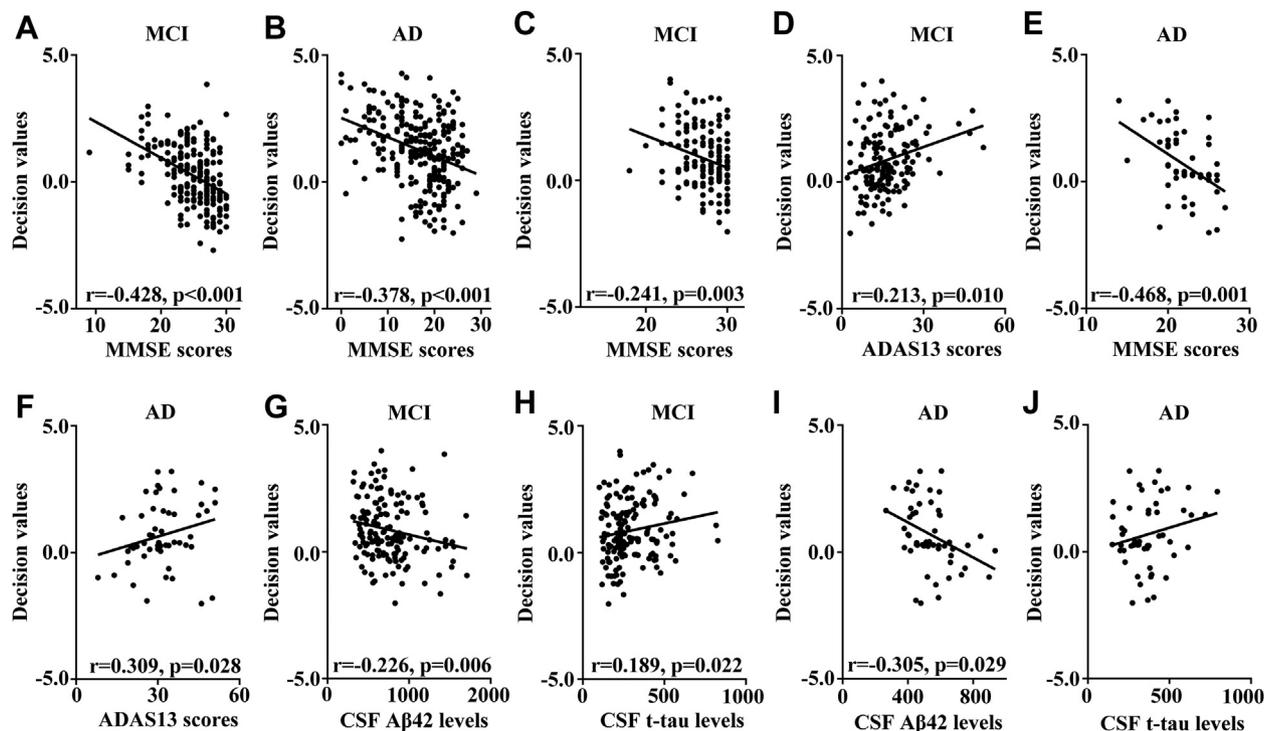

Figure 3. Correlation between the support vector machine model decision values and clinical indices. Mini-Mental State Examination (MMSE) scores of patients with mild cognitive impairment (MCI) **(A)** and patients with Alzheimer's disease (AD) **(B)** in the Multi-Center Alzheimer Disease Imaging dataset. MMSE scores **(C)** and Alzheimer's Disease Assessment Scale 13-item Cognitive Subscale (ADAS13) scores **(D)** of patients with MCI and MMSE scores **(E)** and ADAS13 scores **(F)** of patients with AD in the Alzheimer's Disease Neuroimaging Initiative dataset. Cerebrospinal fluid (CSF) amyloid-β 42 (Aβ42) levels **(G)** and CSF total tau (t-tau) **(H)** levels of patients with MCI and CSF Aβ42 levels **(I)** and CSF t-tau **(J)** levels of patients with AD in the Alzheimer's Disease Neuroimaging Initiative dataset.

Episodic Memory–Related Imaging Features of AD

consistently distinguished between patients with MCI and NC subjects in several datasets with moderate accuracy and also showed excellent diagnostic performance for AD. The episodic memory–related regions identified using RVR showed significantly different SUVRs among the AD, MCI, and NC groups. Importantly, the classification outputs showed a strong association with the cognitive assessments and levels of CSF biomarkers in patients with MCI/AD. Taken together, these comprehensive sets of results indicated that the imaging biomarkers could predict episodic memory impairment and contribute to identifying MCI/AD.

Using the RVR method, 50 episodic memory–related MRI features were identified at the individual level that were mainly distributed in the DMN, LN, and ventral attention network. Also, 19 of these features that localized to the DMN and LN showed better classification performance in the SVM model. The DMN is primarily implicated in episodic memory retrieval and deactivated during the processing of external stimuli in cognitively demanding tasks (59,60). Furthermore, the DMN system, especially the medial temporal lobe subsystem, is frequently disrupted in AD and correlates with disease severity (61,62). The brain regions comprising the DMN and areas with high Aβ load also show considerable overlap, and subjects with positive ^{11}C Pittsburgh Compound B PET scans showed significantly lower resting-state FC in the DMN compared with subjects with negative ^{11}C Pittsburgh Compound B PET scans (63–65). Furthermore, the limbic region of patients with AD exhibits significant gray matter atrophy and accumulation of phosphorylated tau protein, which likely influences the behavioral, emotional, and memory-processing functions of this system (66). Pini et al. found that subjects with late-onset AD have greater memory dysfunction and significantly reduced FC in the LN, indicating a significant association between limbic network FC and memory composite score (67). Altogether, simultaneous impairment of multiple brain networks in MCI/AD subjects can result in abnormal episodic memory function.

Compared with the previous studies that used the RVR method (55,68,69), the combination of multimodal MRI data provided greater prediction performance and more clinical information that included the potential value of these MRI features to differentiate between patients with MCI/AD and NC subjects. In addition, Long et al. (70) reported a valid SVM-based model including structural and functional MRI features that distinguished MCI subjects from healthy subjects with 96.67% accuracy; however, this classifier may have low generalizability owing to the small sample size. In our study, the classification model achieved higher accuracy in the discovery as well as the multicenter validation datasets, which suggests better generalization. Furthermore, principal component analysis could be used for dimensionality reduction during feature selection (71), and some studies used significantly different features between groups for building classifiers (72). However, we selected episodic memory–related MRI features for the SVM model to increase the diagnostic specificity for AD, which was also supported by the results.

To validate the diagnostic utility of MRI indicators in AD, it is necessary to demonstrate the relationship between these indicators and the pathology markers of AD. In this study, most episodic memory–related regions overlapped with sites of Aβ deposition in patients with MCI/AD, which suggested that RVR captured episodic memory–related regions with a solid neurobiological basis. We also observed a significant correlation between the classification outputs and MMSE and Alzheimer's Disease Assessment Scale 13-item Cognitive Subscale scores, indicating that the probability of MCI/AD diagnosis depends on the degree of cognitive impairment. Likewise, a strong correlation between the classification outputs and the levels of the pathological biomarker in the CSF in patients with MCI and patients with AD indicated that the diagnostic model performed better with higher disease risk. Consequently, our findings illustrate a potential association between brain MRI and the personalized clinical features of AD.

Additionally, an episodic memory function prediction model and an episodic memory–related classification model based on the MRI data were proposed in this study. On one hand, for the prediction model, individual episodic memory function could be assessed accurately and conveniently in a clinical setting using objective MRI markers. On the other hand, the proposed model achieved good results in detecting important episodic memory–related regions and building the classification model for diagnosing MCI and AD. In particular, the present classification model was validated in 3 multicenter databases, where it was found to have good generalization and specificity. Thus, it may be used as a promising prescreening tool for identifying individuals with potential risk for AD.

Several limitations in our study ought to be considered. First, as fewer patients with AD had complete episodic memory assessments, the RVR prediction model was constructed in patients with aMCi who presented with relatively mild episodic memory impairment. Second, fractional ALFF data were not used in the present study, as fractional ALFFs were suboptimal for predicting the episodic memory status in our preliminary study, which may result in some underlying information (e.g., unique frequency variance associated with the resting-state band) not being presented. Furthermore, other MRI measures [e.g., FC (52,73), functional network (53), amplitude (47)] may be able to better capture variability in the resting-state data and provide better performance to predict episodic memory score. We will investigate these potential MRI indicators in a subsequent study and assess their clinical utility for early diagnosis of AD. Third, our model effectively diagnosed AD in 2 multicenter datasets but showed relatively lower accuracy in distinguishing between patients with MCI and NC subjects. One possible reason is the heterogeneity of diagnosis of MCI. Another possible reason is that the variations in acquisition methods and the distribution of features between datasets may obfuscate the performance across independent sites/ethnicity validations. Thus, the classification model should be further validated in other subjects with MCI screened strictly according to the A/T/N criteria (3). Additional clinical data (e.g., genetic information) should also be incorporated to improve the classification performance of MCI. Fourth, the clinical value of the present MRI feature classifiers will be assessed in our future study by comparing other non-MRI measures, such as the measurement of blood-related indicators. Fifth, owing to the paucity of clinical information in the MCADI dataset, the neurobiological value of the classification model was assessed with the ADNI dataset. Finally, it is unclear whether these episodic memory–related features can predict the progression of disease owing to the lack of

longitudinal data. Nevertheless, our findings provide novel insights into the neuroimaging features and present a noninvasive method to identify AD.

Conclusions

The combination of functional and structural MRI data can quantitatively and accurately predict episodic memory status in individual patients with aMCI based on a multivariate RVR algorithm, and the objective episodic memory–related MRI features can be used as a diagnostic aid for distinguishing patients with MCI/AD from NC subjects. In addition, the neurobiological interpretability of the classification outputs can further facilitate the application of a classification model for AD.

ARTICLE INFORMATION

From the Department of Neurology (YS, ZW, PiaC, HS, LihG, LijG, QW, CX, ZZ), Affiliated ZhongDa Hospital, School of Medicine, Institution of Neuropsychiatry, Southeast University, Nanjing; School of Life Science and Technology (ZZ), The Key Laboratory of Developmental Genes and Human Disease, Southeast University, Nanjing; Brainnetome Center and National Laboratory of Pattern Recognition (PinC, KZ, YL) and Center for Excellence in Brain Science and Intelligence Technology (YL), Institute of Automation, Chinese Academy of Sciences, Beijing; University of Chinese Academy of Sciences (PinC, YL), Beijing; School of Biological Science and Medical Engineering (KZ), Beihang University, Beijing; and School of Artificial Intelligence (YL), Beijing University of Posts and Tecommunications, Beijing; Department of Psychology (HoZ, ZZ), Xinxiang Medical University, Xinxiang; and Second Affiliated Hospital of Xinxiang Medical University (HoZ, HaZ, ZZ), Xinxiang, China.

YS and ZW contributed equally to this work.

Address correspondence to Zhijun Zhang, Ph.D., at janemengzhang@vip.163.com, or Yong Liu, Ph.D., at yongliu@bupt.edu.cn.

Received Oct 19, 2020; revised and accepted Dec 16, 2020.

Supplementary material cited in this article is available online at https://doi.org/10.1016/j.bpsc.2020.12.007.

REFERENCES

1. Lane CA, Hardy J, Schott JM (2018): Alzheimer's disease. Eur J Neurol 25:59–70.
2. Chehrehnegar N, Nejati V, Shati M, Rashedi V, Lotfi M, Adelirad F, et al. (2020): Early detection of cognitive disturbances in mild cognitive impairment: A systematic review of observational studies. Psychogeriatrics 20:212–228.
3. Cummings J (2019): The National Institute on Aging-Alzheimer's Association Framework on Alzheimer's disease: Application to clinical trials. Alzheimers Dement 15:172–178.
4. Tulving E (2002): Episodic memory: From mind to brain. Annu Rev Psychol 53:1–25.
5. Chen J, Zhang Z, Li S (2015): Can multi-modal neuroimaging evidence from hippocampus provide biomarkers for the progression of amnestic mild cognitive impairment? Neurosci Bull 31:128–140.
6. Gu L, Zhang Z (2019): Exploring structural and functional brain changes in mild cognitive impairment: A whole brain ALE meta-analysis for multimodal MRI. ACS Chem Neurosci 10:2823–2829.
7. McDonough IM, Festini SB, Wood MM (2020): Risk for Alzheimer's disease: A review of long-term episodic memory encoding and retrieval fMRI studies. Ageing Res Rev 62:101133.
8. Bai F, Zhang Z, Watson DR, Yu H, Shi Y, Yuan Y, et al. (2009): Abnormal functional connectivity of hippocampus during episodic memory retrieval processing network in amnestic mild cognitive impairment. Biol Psychiatry 65:951–958.
9. Terry DP, Sabatinelli D, Puente AN, Lazar NA, Miller LS (2015): A meta-analysis of fMRI activation differences during episodic memory in Alzheimer's disease and mild cognitive impairment. J Neuroimaging 25:849–860.
10. Schwindt GC, Black SE (2009): Functional imaging studies of episodic memory in Alzheimer's disease: A quantitative meta-analysis. Neuroimage 45:181–190.
11. Wang C, Pan Y, Liu Y, Xu K, Hao L, Huang F, et al. (2018): Aberrant default mode network in amnestic mild cognitive impairment: A meta-analysis of independent component analysis studies. Neurol Sci 39:919–931.
12. Sartori JM, Reckziegel R, Passos IC, Czepielewski LS, Fijtman A, Sodre LA, et al. (2018): Volumetric brain magnetic resonance imaging predicts functioning in bipolar disorder: A machine learning approach. J Psychiatr Res 103:237–243.
13. Siegel JS, Ramsey LE, Snyder AZ, Metcalf NV, Chacko RV, Weinberger K, et al. (2016): Disruptions of network connectivity predict impairment in multiple behavioral domains after stroke. Proc Natl Acad Sci U S A 113:E4367–E4376.
14. Feng C, Cui Z, Cheng D, Xu R, Gu R (2019): Individualized prediction of dispositional worry using white matter connectivity. Psychol Med 49:1999–2008.
15. Mwangi B, Wu MJ, Cao B, Passos IC, Lavagnino L, Keser Z, et al. (2016): Individualized prediction and clinical staging of bipolar

disorders using neuroanatomical biomarkers. Biol Psychiatry Cogn Neurosci Neuroimaging 1:186–194.

16. Tipping ME (2001): Sparse Bayesian learning and the relevance vector machine. J Mach Learn Res 1:211–244.

17. Cui Z, Gong G (2018): The effect of machine learning regression algorithms and sample size on individualized behavioral prediction with functional connectivity features. Neuroimage 178:622–637.

18. Wang Y, Fan Y, Bhatt P, Davatzikos C (2010): High-dimensional pattern regression using machine learning: From medical images to continuous clinical variables. Neuroimage 50:1519–1535.

19. Viviano JD, Buchanan RW, Calarco N, Gold JM, Foussias G, Bhagwat N, et al. (2018): Resting-state connectivity biomarkers of cognitive performance and social function in individuals with schizophrenia spectrum disorder and healthy control subjects. Biol Psychiatry 84:665–674.

20. So JH, Madusanka N, Choi HK, Choi BK, Park HG (2019): Deep learning for Alzheimer's disease classification using texture features. Curr Med Imaging Rev 15:689–698.

21. Lin W, Gao Q, Yuan J, Chen Z, Feng C, Chen W, et al. (2020): Predicting Alzheimer's disease conversion from mild cognitive impairment using an extreme learning machine-based grading method with multimodal data. Front Aging Neurosci 12:77.

22. Ezzati A, Zammit AR, Harvey DJ, Habeck C, Hall CB, Lipton RB, et al. (2019): Optimizing machine learning methods to improve predictive models of Alzheimer's disease. J Alzheimers Dis 71:1027–1036.

23. Popuri K, Ma D, Wang L, Beg MF (2020): Using machine learning to quantify structural MRI neurodegeneration patterns of Alzheimer's disease into dementia score: Independent validation on 8,834 images from ADNI, AIBL, OASIS, and MIRIAD databases. Hum Brain Mapp 41:e25115.

24. Wang L, Liu Y, Zeng X, Cheng H, Wang Z, Wang Q (2020): Region-of-interest based sparse feature learning method for Alzheimer's disease identification. Comput Methods Programs Biomed 187:105290.

25. Shahamat H, Saniee Abadeh M (2020): Brain MRI analysis using a deep learning based evolutionary approach. Neural Netw 126:218–234.

26. Toshkhujaev S, Lee KH, Choi KY, Lee JJ, Kwon GR, Gupta Y, et al. (2020): Classification of Alzheimer's disease and mild cognitive impairment based on cortical and subcortical features from MRI T1 brain images utilizing four different types of datasets. J Healthc Eng 2020:3743171.

27. Zheng W, Cui B, Sun Z, Li X, Han X, Yang Y, et al. (2020): Application of generalized split linearized Bregman iteration algorithm for Alzheimer's disease prediction. Aging (Albany NY) 12:6206–6224.

28. Basaia S, Agosta F, Wagner L, Canu E, Magnani G, Santangelo R, et al. (2019): Automated classification of Alzheimer's disease and mild cognitive impairment using a single MRI and deep neural networks. Neuroimage Clin 21:101645.

29. Wee CY, Liu C, Lee A, Poh JS, Ji H, Qiu A, et al. (2019): Cortical graph neural network for AD and MCI diagnosis and transfer learning across populations. Neuroimage Clin 23:101929.

30. Wang Y, Xu C, Park JH, Lee S, Stern Y, Yoo S, et al. (2019): Diagnosis and prognosis of Alzheimer's disease using brain morphometry and white matter connectomes. Neuroimage Clin 23:101859.

31. Gupta Y, Lee KH, Choi KY, Lee JJ, Kim BC, Kwon GR, et al. (2019): Early diagnosis of Alzheimer's disease using combined features from voxel-based morphometry and cortical, subcortical, and hippocampus regions of MRI T1 brain images. PLoS One 14:e0222446.

32. Frenzel S, Wittfeld K, Habes M, Klinger-Konig J, Bulow R, Volzke H, et al. (2019): A biomarker for Alzheimer's disease based on patterns of regional brain atrophy. Front Psychiatry 10:953.

33. Liu CF, Padhy S, Ramachandran S, Wang VX, Efimov A, Bernal A, et al. (2019): Using deep Siamese neural networks for detection of brain asymmetries associated with Alzheimer's disease and mild cognitive impairment. Magn Reson Imaging 64:190–199.

34. Duraisamy B, Shanmugam JV, Annamalai J (2019): Alzheimer disease detection from structural MR images using FCM based weighted probabilistic neural network. Brain Imaging Behav 13:87–110.

35. Bhagwat N, Viviano JD, Voineskos AN, Chakravarty MM, Alzheimer's Disease Neuroimaging Initiative (2018): Modeling and prediction of clinical symptom trajectories in Alzheimer's disease using longitudinal data. PLoS Comput Biol 14:e1006376.

36. Samper-Gonzalez J, Burgos N, Bottani S, Fontanella S, Lu P, Marcoux A, et al. (2018): Reproducible evaluation of classification methods in Alzheimer's disease: Framework and application to MRI and PET data. Neuroimage 183:504–521.

37. Sorensen L, Igel C, Pai A, Balas I, Anker C, Lillholm M, et al. (2017): Differential diagnosis of mild cognitive impairment and Alzheimer's disease using structural MRI cortical thickness, hippocampal shape, hippocampal texture, and volumetry. Neuroimage Clin 13:470–482.

38. Previtali F, Bertolazzi P, Felici G, Weitschek E (2017): A novel method and software for automatically classifying Alzheimer's disease patients by magnetic resonance imaging analysis. Comput Methods Programs Biomed 143:89–95.

39. Sorensen L, Igel C, Liv Hansen N, Osler M, Lauritzen M, Rostrup E, et al. (2016): Early detection of Alzheimer's disease using MRI hippocampal texture. Hum Brain Mapp 37:1148–1161.

40. Jin D, Zhou B, Han Y, Ren J, Han T, Liu B, et al. (2020): Generalizable, reproducible, and neuroscientifically interpretable imaging biomarkers for Alzheimer's disease. Adv Sci (Weinh) 7:2000675.

41. Folstein MF, Folstein SE, McHugh PR (1975): "Mini-mental state." A practical method for grading the cognitive state of patients for the clinician. J Psychiatr Res 12:189–198.

42. Savage RM, Gouvier WD (1992): Rey Auditory-Verbal Learning Test: The effects of age and gender, and norms for delayed recall and story recognition trials. Arch Clin Neuropsychol 7:407–414.

43. Knopman DS, Lundt ES, Therneau TM, Vemuri P, Lowe VJ, Kantarci K, et al. (2019): Entorhinal cortex tau, amyloid-beta, cortical thickness and memory performance in non-demented subjects. Brain 142:1148–1160.

44. Shin MS, Park SY, Park SR, Seol SH, Kwon JS (2006): Clinical and empirical applications of the Rey-Osterrieth Complex Figure Test. Nat Protoc 1:892–899.

45. Shi Y, Gu L, Wang Q, Gao L, Zhu J, Lu X, et al. (2020): Platelet amyloid-beta protein precursor (AbetaPP) ratio and phosphorylated tau as promising indicators for early Alzheimer's disease. J Gerontol A Biol Sci Med Sci 75:664–670.

46. Shi Y, Lu X, Zhang L, Shu H, Gu L, Wang Z, et al. (2019): Potential value of plasma amyloid-beta, total tau, and neurofilament light for identification of early Alzheimer's disease. ACS Chem Neurosci 10:3479–3485.

47. Li JC, Jin D, Li A, Liu B, Song CY, Wang P, et al. (2019): ASAF: Altered spontaneous activity fingerprinting in Alzheimer's disease based on multisite fMRI. Science Bulletin 64:998–1010.

48. Zhao K, Ding YH, Han Y, Fan Y, Alexander-Bloch AF, Han T, et al. (2020): Independent and reproducible hippocampal radiomic biomarkers for multisite Alzheimer's disease: Diagnosis, longitudinal progress and biological basis. Science Bulletin 65:1103–1113.

49. Yan CG, Chen X, Li L, Castellanos FX, Bai TJ, Bo QJ, et al. (2019): Reduced default mode network functional connectivity in patients with recurrent major depressive disorder. Proc Natl Acad Sci U S A 116:9078–9083.

50. Hansson O, Seibyl J, Stomrud E, Zetterberg H, Trojanowski JQ, Bittner T, et al. (2018): CSF biomarkers of Alzheimer's disease concord with amyloid-beta PET and predict clinical progression: A study of fully automated immunoassays in BioFINDER and ADNI cohorts. Alzheimers Dement 14:1470–1481.

51. Fan L, Li H, Zhuo J, Zhang Y, Wang J, Chen L, et al. (2016): The Human Brainnetome Atlas: A new brain atlas based on connectional architecture. Cereb Cortex 26:3508–3526.

52. Jin D, Wang P, Zalesky A, Liu B, Song C, Wang D, et al. (2020): Grab-AD: Generalizability and reproducibility of altered brain activity and diagnostic classification in Alzheimer's disease. Hum Brain Mapp 41:3379–3391.

53. Liu Y, Yu C, Zhang X, Liu J, Duan Y, Alexander-Bloch AF, et al. (2014): Impaired long distance functional connectivity and weighted network architecture in Alzheimer's disease. Cereb Cortex 24:1422–1435.

54. Gong Q, Li L, Du M, Pettersson-Yeo W, Crossley N, Yang X, et al. (2014): Quantitative prediction of individual psychopathology in trauma

survivors using resting-state fMRI. Neuropsychopharmacology 39:681–687.

55. Zhu J, Zhu DM, Zhang C, Wang Y, Yang Y, Yu Y (2019): Quantitative prediction of individual cognitive flexibility using structural MRI. Brain Imaging Behav 13:781–788.

56. Hsu CW, Lin CJ (2002): A comparison of methods for multiclass support vector machines. IEEE Trans Neural Netw 13:415–425.

57. Noble WS (2006): What is a support vector machine? Nat Biotechnol 24:1565–1567.

58. Xie Y, Cui Z, Zhang Z, Sun Y, Sheng C, Li K, et al. (2015): Identification of amnestic mild cognitive impairment using multi-modal brain features: A combined structural MRI and diffusion tensor imaging study. J Alzheimers Dis 47:509–522.

59. Buckner RL, Andrews-Hanna JR, Schacter DL (2008): The brain's default network: Anatomy, function, and relevance to disease. Ann N Y Acad Sci 1124:1–38.

60. Buckner RL, DiNicola LM (2019): The brain's default network: Updated anatomy, physiology and evolving insights. Nat Rev Neurosci 20:593–608.

61. Qi H, Liu H, Hu H, He H, Zhao X (2018): Primary disruption of the memory-related subsystems of the default mode network in Alzheimer's disease: Resting-state functional connectivity MRI study. Front Aging Neurosci 10:344.

62. Chhatwal JP, Schultz AP, Johnson K, Benzinger TL, Jack C Jr, Ances BM, et al. (2013): Impaired default network functional connectivity in autosomal dominant Alzheimer disease. Neurology 81:736–744.

63. Adriaanse SM, Sanz-Arigita EJ, Binnewijzend MA, Ossenkoppele R, Tolboom N, van Assema DM, et al. (2014): Amyloid and its association with default network integrity in Alzheimer's disease. Hum Brain Mapp 35:779–791.

64. Sheline YI, Raichle ME, Snyder AZ, Morris JC, Head D, Wang S, et al. (2010): Amyloid plaques disrupt resting state default mode network connectivity in cognitively normal elderly. Biol Psychiatry 67:584–587.

65. Sperling RA, Laviolette PS, O'Keefe K, O'Brien J, Rentz DM, Pihlajamaki M, et al. (2009): Amyloid deposition is associated with impaired default network function in older persons without dementia. Neuron 63:178–188.

66. Mattsson N, Insel PS, Donohue M, Jogi J, Ossenkoppele R, Olsson T, et al. (2019): Predicting diagnosis and cognition with (18)F-AV-1451 tau PET and structural MRI in Alzheimer's disease. Alzheimers Dement 15:570–580.

67. Pini L, Geroldi C, Galluzzi S, Baruzzi R, Bertocchi M, Chito E, et al. (2020): Age at onset reveals different functional connectivity abnormalities in prodromal Alzheimer's disease. Brain Imaging Behav 14:2594–2605.

68. Stonnington CM, Chu C, Kloppel S, Jack CR Jr, Ashburner J, Frackowiak RS, et al. (2010): Predicting clinical scores from magnetic resonance scans in Alzheimer's disease. Neuroimage 51:1405–1413.

69. Moradi E, Hallikainen I, Hanninen T, Tohka J, Alzheimer's Disease Neuroimaging Initiative (2017): Rey's Auditory Verbal Learning Test scores can be predicted from whole brain MRI in Alzheimer's disease. Neuroimage Clin 13:415–427.

70. Long Z, Jing B, Yan H, Dong J, Liu H, Mo X, et al. (2016): A support vector machine-based method to identify mild cognitive impairment with multi-level characteristics of magnetic resonance imaging. Neuroscience 331:169–176.

71. Yang W, Lui RL, Gao JH, Chan TF, Yau ST, Sperling RA, et al. (2011): Independent component analysis-based classification of Alzheimer's disease MRI data. J Alzheimers Dis 24:775–783.

72. Zheng Y, Guo H, Zhang L, Wu J, Li Q, Lv F (2019): Machine learning-based framework for differential diagnosis between vascular dementia and Alzheimer's disease using structural MRI features. Front Neurol 10:1097.

73. Teipel SJ, Metzger CD, Brosseron F, Buerger K, Brueggen K, Catak C, et al. (2018): Multicenter resting state functional connectivity in prodromal and dementia stages of Alzheimer's disease. J Alzheimers Dis 64:801–813.